Modelling the Wetting and Cooking of a Single Cereal Grain

M.J. McGuinness[*], C.P. Please[†], N. Fowkes[‡], P. McGowan[§], L. Ryder[¶], D. Forte[||]

Abstract

Three models are presented for the wetting of whole grains of cereal. Two are for temperatures below gelatinisation temperatures, one of which incorporates the effects of swelling of the grain. A third model is presented for wetting of a grain at temperatures above gelatinisation, and hence cooking the grain. The models are developed as partial differential equations, and solved in a variety of ways. A model that ignores swelling at temperatures below gelatinisation is solved for wetting times by using the concept of mean action time, which reduces the problem to an exactly solvable linear Poisson equation. The other two models, which include swelling and cooking respectively, are solved approximately, taking advantage of the steep nonlinear diffusion fronts that develop. The aim of the modelling is to improve understanding of the cooking of whole grain cereals prior to processing into breakfast cereals. Moisture penetration curves are obtained and compared. Regions where penetration rate is approximately linear are noted, suggesting that nonlinear diffusion equations are a promising way to model grain wetting and cooking.

Keywords: cooking cereals, nonlinear diffusion, swelling, Stefan.

[*]School of Mathematical and Computer Science, Victoria University of Wellington, PO Box 600, Wellington, New Zealand

[†]Department of Mathematics, University of Southampton, Southampton, England SO17 1BJ

[‡]Department of Mathematics, University of Western Australia, Nedlands, WA 6907, Australia

[§]Orica Engineering, 1 Nicholson St., Melbourne, Vic 3000, Australia

[¶]Uncle Tobys Company Ltd - Research, PO Box 175, Rutherglen, Vic 3685, Australia

[||]Uncle Tobys Company Ltd - Research, PO Box 175, Rutherglen, Vic 3685, Australia

1 Introduction

Whole grains of corn, wheat, oats and rice are traditionally prepared commercially for processing into breakfast cereals by cooking in one tonne batches in a rotating steam pressure-cooker. Cooking requires two processes, heating the grain to a high enough temperature (gelatinisation temperature), and hydrating the grain to a high enough moisture content. After cooking, the grains are dried, flaked, toasted and coated before packaging as a finished breakfast cereal product. The quality of the finished product depends on how evenly the whole grains are cooked before processing further.

In this paper we describe and solve two models of the hydrating process at lower temperatures, one that excludes and one that includes the effects of swelling, and a third simple model of hydrating at gelatinisation temperatures. The modelling is intended to improve understanding of grain wetting, so that better control may be exercised over the cooking process. Grain wetting is a slower process than grain heating, so we focus on this aspect of grain cooking.

Gelatinisation is the process whereby water and heat cause starch granules to swell, and eventually burst. We take a simplified view of this complicated process, which is described in some detail in Stapley (1995). Swelling is reversible for temperatures below the gelatinisation temperature, $T_{\rm gel}$, and is irreversible above $T_{\rm gel}$. Water is taken up by the grain, which swells by a volume nearly equal to that of the water taken up. The water bonds with the starch, although there is evidence that bonded water is still free to interact with neighbouring dry starch.

Gelatinisation is an irreversible reaction between the starch and water which occurs over a narrow temperature range of about 10°C, centered about the temperature $T_{\rm gel}$. Note that this temperature is dependent on the local moisture level. An experimentally derived relationship is illustrated in Figure 1. If moisture content is too low, it is believed that gelatinisation cannot occur at all. The higher the moisture content, the lower the temperature at which gelatinisation occurs. In the majority of this paper we consider the case where the temperature is below gelatinisation. A simple treatment that includes gelatinisation is presented in section 4. For models and analyses of cooking processes with simultaneous hydrolization and heating, either in steam or boiling

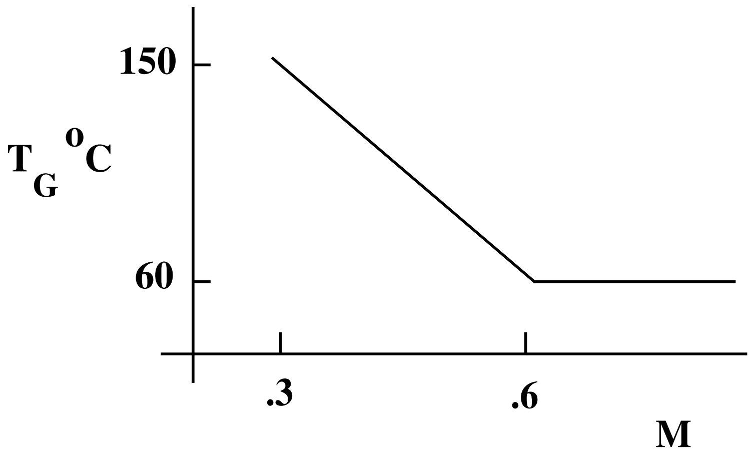

Figure 1: A sketch indicating gelatinisation temperature versus moisture content (dry ratio).

water, see also Stapley (1995) and Stapley *et al* (1997a,b).

Stapley (1995) gives a detailed review of the processes involved in gelatinisation of starch, as well as comparing models of grain wetting. He describes detailed NMR studies of the penetration of moisture into wheat grains, for both steamed grains and grains placed in boiling water. More details are given in the discussion section of this paper.

Suzuki *et al* (1977) investigate soaking and cooking mechanisms for rice. Their soaking model is an empirical algebraic equation describing experimental results. Their cooking model has a shrinking un-cooked core, and conservation of mass principles are applied to set up simple rate equations. Two cases are considered, one in which the rate of cooking is limited by the reaction rate at a sharp cooking front and is assumed proportional to the concentration differences across the front, and the other in which the rate of cooking is limited by the diffusion of water across the cooked region. The analyses presented in this paper extend the work of Suzuki *et al* by including the effects of grain swelling, and by setting up more generally applicable nonlinear diffusion equations which are then approximately solved, with the effects of small parameters and assumptions being more explicit and understandable.

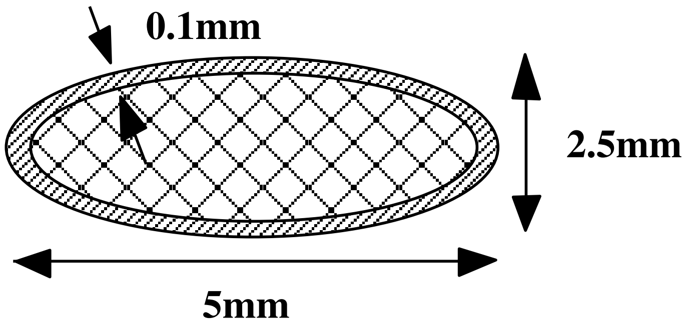

Figure 2: Sketch of a simplified generic grain

Bakshi and Singh (1982) present a model for the simultaneous diffusion of water and starch gelatinisation during rice par-boiling. They fit linear diffusion equations to data, and obtain regression equations for soaking and cooking times, dependent on temperature. Grain swelling is not included. Zhang *et al* (1984) present numerical finite element solutions of a two-dimensional nonlinear diffusion equation with swelling included, for soaking rice grains.

2 Modelling

A typical generic grain structure is shown in Figure 2. Two major parts of the grain are identified in a simplified view of the actual grain, the outer cellulose skin or pericarp, and the inner region filled with starch granules. For the purposes of our modelling here we neglect the pericarp as it is so thin that it has little influence on the moisture transport. We take the starch granules to form a single homogeneous material. Note that in doing this we will not be investigating the effect of the crease in wheat grains, which is known to provide a possible preferred path for the moisture (Stapley, 1995).

Properties	**Cellulose**	**Corn Starch**	**units**
specific heat c_p	2500	2160	J/(kg °K)
density ρ	950	1400	kg/m^3
thermal conductivity κ	0.15	0.26	W/(m °K)
thermal diffusivity k	6.3×10^{-8}	8.6×10^{-8}	m^2/s
lengthscale	0.1 – 0.15	1.25	mm

Table 1: Some thermal properties of whole grains

2.1 Heat Transport

Heat is transported within the grain primarily by conduction with the latent heat related to chemical changes within the grain being negligible. The heat flow can be adequately modelled by a simple linear diffusion equation. Typical values for the parameters associated with the thermal problem are given in Table 1. The time for the heat to equilibrate across the grain can therefore be easily estimated. For a corn grain this is found to be around 6 seconds and other grains all have a similar small thermal time response. The hydration of the grain is much slower and so for the purposes of modelling moisture transport we consider the grain to be isothermal. Stapley *et al* (1997b) also note the rapidity of heat conduction in wheat grains, compared to moisture penetration rates.

2.2 Moisture Transport

Water motion within the grain is primarily due to sorption processes, driven by a chemical potential called water affinity. As the water moves into the starch so the grain swells in almost equal volume to the volume of water absorbed. Related modelling has been conducted on the sorption of solvent by polymers (Thomas and Windle, 1982) — starch is a natural polymer.

In describing the state of the grain the concept of moisture content, denoted by M, will be used. M is known as the *dry ratio*, and is the ratio of the mass of water to the mass of dry grain.

The paper by Syarief *et al* (1987) describes experimental work that was performed to determine how water moves in whole grains at temperatures below T_{gel}. They present the results of careful experiments on the uptake and loss of moisture from various parts of a corn kernel, and fit the experimental results to numerical solutions of a nonlinear diffusion equation. They assume that the following equation describes the uptake of moisture at 40°C:

$$\frac{\partial M}{\partial t'} = \nabla \cdot (D \nabla M) \ . \tag{1}$$

The data is adequately fitted with the function

$$D \equiv D_0 e^{\delta M}, \tag{2}$$

where D_0 and δ are positive real constants. For corn starch, the values they find for D_0 and δ at 40°C suggest an average value (for floury and horny endosperm)

$$D = 1.5 \times 10^{-11} e^{8.6M} \ \ \text{m}^2/\text{s} \ . \tag{3}$$

In interpreting this data we should note that the experiments are automatically affected by swelling, so that the fitted value of diffusivity has swelling built into it. As noted in Philip (1969), Broadbridge (1990) and Smiles and Rosenthal (1968), in the context of swelling soils, accounting for swelling in a wetting environment must be done carefully with particular attention paid to the difference between the dry ratio and the wet ratio as appropriate variables. For the purposes of this paper we shall simply take the data given above as an indication that the diffusivity is a strong exponential function of the moisture content. The detailed values of the coefficients within the diffusivity will not be exploited except as illustrative examples.

It should be noted that a similar expression, with strong exponential dependency of the diffusion coefficient on moisture content, is used in the modelling of the diffusion of solvent due to solvent activity in glassy polymers (Thomas and Windle, 1982). Starch is a naturally occuring polymer, which is believed to undergo a glassy transition during gelatinisation.

2.2.1 Grain swelling

Noting that the swelling of materials as fluids are absorbed has been considered in soil wetting (Philip, 1969; Broadbridge, 1990; Smiles and Rosenthal, 1968) and solvent penetration of polymers (Thomas and Windle, 1982), we give here an outline derivation of the underlying equations indicating the approximations made.

The water occupies a volume fraction ϕ while the solids of the grain, mostly starch, occupy a volume fraction $1-\phi$. We use Eulerian coordinates, fixed in space.

We follow Bear (1972) in defining at each point in the grain an average fluid velocity $\mathbf{u}_w$, averaged over the void space of a representative elementary volume of grain, and an analogous average solid grain velocity $\mathbf{u}_s$. We assume constant densities of water and solid grain, so that conservation of mass corresponds to conservation of volume, and gives

$$\frac{\partial(1-\phi)}{\partial t} + \nabla \cdot (\mathbf{u}_s(1-\phi)) = 0 \ , \tag{4}$$

$$\frac{\partial \phi}{\partial t} + \nabla \cdot (\mathbf{u}_w \phi) = 0 \ . \tag{5}$$

Adding and subtracting these gives

$$\nabla \cdot ((\mathbf{u}_w - \mathbf{u}_s)\phi + \mathbf{u}_s) = 0 \ , \tag{6}$$

$$2\frac{\partial \phi}{\partial t} + \nabla \cdot ((\mathbf{u}_w + \mathbf{u}_s)\phi - \mathbf{u}_s) = 0 \ . \tag{7}$$

We take the average velocity $\mathbf{u}_w$ of the water to be driven by gradients in the water affinity as described previously. From equation (1) the flux of M, relative to stationary solid, at any point is

$$-D_0 e^{\delta M} \nabla M$$

and hence, noting the general form for conservation laws in Bear (1972), the average velocity of the water relative to a stationary solid grain is

$$-D_0 e^{\delta M} \frac{\nabla M}{M} \ . \tag{8}$$

This gives

$$\mathbf{u}_w = \mathbf{u}_s - D_0 e^{\delta M} \frac{\nabla M}{M} \ , \tag{9}$$

a relationship between average water and solid velocities. Substituting this expression for average water velocity into the conservation equations gives

$$\nabla \cdot \left(-D_0 e^{\delta M} \frac{\nabla M}{M} \phi + \mathbf{u}_s \right) = 0, \tag{10}$$

$$2 \frac{\partial \phi}{\partial t} + \nabla \cdot \left(-D_0 e^{\delta M} \frac{\nabla M}{M} \phi + (2\phi - 1) \mathbf{u}_s \right) = 0\ . \tag{11}$$

Note that

$$M = \frac{\rho_w \phi}{\rho_s (1 - \phi)} \tag{12}$$

where ρ_w and ρ_s are the densities of water and solid. We use $\rho_w = 992$ kg/m^3 at 40°C when illustrating with parameter values in this paper.

The model is complete except for the fact that we have stated nothing about the forces acting on the solid that may result due to its motion. Models may either take the solid as a visco-elastic material or some other behaviour based on the properties of the grain. Such models have been considered by several authors, for instance King (1989) and Thomas and Windle (1982).

In this paper we shall, however, consider simple symmetric geometries where the forces do not need to be considered (although in practice the forces may make the resulting flow unstable through buckling). Assuming there is no vorticity in the water flow generated by the swelling, equation (10) can be integrated to give

$$D_0 e^{\delta M} \frac{\phi}{M} \nabla M = \mathbf{u}_s\ . \tag{13}$$

Substituting this into equation 11 gives the equation of motion for the water in the swelling grain,

$$\frac{\partial \phi}{\partial t} = \nabla \cdot \left((1 - \phi) D_0 e^{\delta M} \frac{\nabla M}{M} \phi \right)\ . \tag{14}$$

Using the relationship (12) between M and ϕ this equation can be written in terms of either. Hence equation (14) becomes

$$\frac{\partial}{\partial t} \left(\frac{M}{1 + (\rho_s/\rho_w) M} \right) = \nabla \cdot \left(\frac{D_0 e^{\delta M} \nabla M}{[1 + (\rho_s/\rho_w) M]^2} \right) \tag{15}$$

or in terms of the other variable

$$\frac{\partial \phi}{\partial t} = \nabla \cdot \left(D_0 e^{\left(\frac{\delta \rho_w \phi}{\rho_s (1-\phi)}\right)} \nabla \phi \right) \ . \tag{16}$$

The fact that ϕ satisfies a nonlinear diffusion equation is also noted for swelling soils in Philip (1969), Broadbridge (1990) and Smiles and Rosenthal (1968).

This swelling model requires, in addition to the initial and boundary conditions on the moisture, a boundary condition on the outer surface stating that it will move at a velocity given by

$$D_0 e^{\delta M} \frac{\phi}{M} \nabla M \cdot \mathbf{n}$$

where $\mathbf{n}$ is the outward facing normal to the surface. The problem is therefore a moving boundary problem for a nonlinear diffusion equation.

Note that this model gives the no-swelling problem of equations (1) and (2) in the asymptotic limit where $M = O(1)$ and $\rho_s/\rho_w \to 0$.

2.2.2 The nondimensional problem

Consider the grain to be initially at some uniform low moisture content M_0 which is typically about 0.15. The outer surface is taken to be in a water bath and the surface moisture content is taken to be M_1, determined by the saturation point where the moisture activity reaches the value one, which usually corresponds to M_1 around 0.6. The problem can then be non-dimensionalised by taking

$$\bar{\mathbf{x}} = \mathbf{x}/L \ ,$$

$$m = \frac{M - M_1}{M_1 - M_0} \quad , \qquad \bar{t} = \frac{D_0}{L^2} e^{\delta M_1} t \ .$$

where L is the lengthscale of the grain. In the remainder of the paper the over-bar notation will be neglected for simplicity. Hence (15) becomes

$$\frac{\partial}{\partial t} \left(\frac{\alpha + m}{\gamma + \nu m} \right) = \nabla \cdot \left(\frac{e^{\beta m} \nabla m}{(\gamma + \nu m)^2} \right) \tag{17}$$

with

$$
\begin{aligned}
m &= -1 \text{ initially} \quad , & (18)\\
m &= 0 \text{ at the boundary, and} & (19)\\
v_n &= \frac{\nu}{\gamma}\nabla m \cdot \mathbf{n} \quad , & (20)
\end{aligned}
$$

where v_n is the normal velocity of the outer surface and $\mathbf{n}$ is the outward normal to this surface. Finally an initial position for the outer surface must be given. Within these equations the non-dimensional parameters are

$$
\alpha = \frac{M_1}{M_1 - M_0} \quad , \qquad \gamma = 1 + \frac{\rho_s M_1}{\rho_w} \quad ,
$$

$$
\nu = \frac{\rho_s(M_1 - M_0)}{\rho_w} = \frac{\gamma - 1}{\alpha} \quad , \qquad \beta = \delta(M_1 - M_0) \quad .
$$

Hence there are three separate non-dimensional groups to consider.

To illustrate with typical values, we match the diffusivity of the swelling problem (15) with the diffusivity in the equations (1), (2) and (3) found by Syarief *et al* (1987). That is, we match

$$
\frac{D_0 e^{\delta M}}{[1 + (\rho_s/\rho_w)M]^2} = 1.5 \times 10^{-11} e^{8.6M} \tag{21}
$$

with M taking values in the range 0.05–0.35 as used by Syarief *et al*. We find a close match when $D_0 = 1.6 \times 10^{-11}$ and $\delta = 10.8$. The relative difference between both sides of equation (21) is then found to be less than 4% when M is in the range 0.05–0.35.

Then when $M_1 = 0.6$, corresponding values for the swelling problem parameters based on the corn starch properties listed in Table 2 are $\gamma = 1.8$, $\alpha = 1.3$, $\nu = 0.6$, and $\beta = 5$.

Note that the no-swelling problem

$$
\frac{\partial m}{\partial t} = \nabla \cdot \left(e^{\beta m} \nabla m \right) \quad , \tag{22}
$$

with $m = -1$ when $t = 0$, and $m = 0$ on the boundary, is recovered in the case where $\rho_w \to \infty$. This gives $\nu \to 0$ and $\gamma \to 1$. This limiting case of infinite water density can be interpreted to be the limit where the penetrating water occupies no volume (since it has infinite density), and hence there is no swelling of the grain to accommodate the water. Matching this to the results of Syarief *et al* (1987) gives $D_0 = 1.5 \times 10^{-11}$ m^2/s and $\delta = 8.6$.

3 Analysis of moisture transport model

The model given above will now be used to determine the motion of the moisture within the grain. Three approaches will be used to find approximate solutions so that, in particular, the dependency of the time to wet the grain adequately can be seen as a function of the non-dimensional parameters. The first model ignores swelling and assumes temperature is below the gelatinisation temperature T_G, the second model includes swelling but still assumes temperature is below T_G, and the third model allows for both swelling and cooking, with temperature above T_G.

3.1 Mean Action Time Analysis — Non-Swelling Model

To start the analysis we consider the no-swelling limit of the problem (17), namely (22), and use the ideas of mean-action time to derive estimates of the time to wet any given point in the grain. The theory behind this procedure is given by McNabb (1975) and McNabb and Wake (1991), and is outlined briefly here. A mean action time t** is defined at each point x in the grain by

$$t^{**}(x) \equiv \frac{\int_0^\infty t[\frac{\partial}{\partial t}\int_{-1}^m Dds]dt}{\int_0^\infty [\frac{\partial}{\partial t}\int_{-1}^m Dds]dt}. \tag{23}$$

and represents the time taken to wet this point in the grain. When a steep moisture front is present, t** gives the time of arrival of the front at point x. For the diffusivity considered here, $D = D_0 \exp(\delta M)$, the integrals can be simplified to give

$$t^{**}(x) = \frac{\int_0^\infty (1 - e^{\beta m})dt}{1 - e^{-\beta}}. \tag{24}$$

We define

$$\Phi \equiv \frac{1}{\beta}\int_0^\infty (1 - e^{\beta m})dt, \tag{25}$$

so that

$$t^{**} = \frac{\beta\Phi}{1 - e^{-\beta}}, \tag{26}$$

Using equation (22), it can be shown that Φ satisfies a (linear) Poisson equation namely:

$$\nabla^2\Phi = -1, \tag{27}$$

with the boundary condition on the surface of the grain being $\Phi = 0$. The largest value of Φ is denoted by Φ_G, and gives the mean action time for moisture to penetrate the entire grain.

As an example of how this method can be used for the moisture movement in a grain consider an ellipsoidal region for the grain bounded by

$$x^2 + \frac{y^2}{b^2} + \frac{z^2}{c^2} = 1 \quad . \tag{28}$$

Here, (x, y, z) are the non-dimensional spatial variables and $(1, b, c)$ are the non-dimensional semiaxes of the ellipsoid. The solution to the Poisson equation is

$$\Phi = \left[1 - (x^2 + \frac{y^2}{b^2} + \frac{z^2}{c^2})\right] / \left[2\left(1 + \frac{1}{b^2} + \frac{1}{c^2}\right)\right] \tag{29}$$

The contours of moisture are ellipsoids, which move deeper into the grain as time progresses. The variable Φ_G then occurs at the centre of the grain, giving the maximum mean action time

$$t_G^{**} = \frac{\beta}{1 - e^{-\beta}}\Phi_G \quad , \tag{30}$$

where

$$\Phi_G = \frac{1}{2\left(1 + \frac{1}{b^2} + \frac{1}{c^2}\right)} \quad . \tag{31}$$

The term Φ_G can then be seen to be a shape factor, dependent on grain shape. The expression for maximum mean action time **in seconds** is then

$$t'_G = \frac{L^2 e^{-\delta M_1}\beta\Phi_G}{D_0(1 - e^{-\beta})}. \tag{32}$$

Using $D_0 = 1.5 \times 10^{-11}$, $\delta = 8.6$, $M_1 = 0.6$, $M_0 = 0.15$, and the grain shape illustrated in figure 2, leads to a wetting time $t'_G = 8.5$ minutes.

In later sections we will want to compare models, and we have used cylindrical geometry in the second and third models. If cylindrical geometry is used instead of ellipsoidal geometry for this mean action time model, then $b = 1$ and $c \to \infty$, and the mean action time becomes

$$4t^{**} = \frac{\beta}{1 - e^{-\beta}}(1 - s^2) \ , \tag{33}$$

where $s^2 \equiv x^2 + y^2$. This corresponds to a shape factor $\Phi_G = 1/4$, not much different to the value $\Phi_G = 1/4.5$ applying to ellipsoidal grain geometry, suggesting that a cylindrical model will be a good approximation for ellipsoids with aspect ratios similar to that considered here. Detailed comparisons of this non-swelling mean action time model with the other models are made in the Discussion section, for cylindrical geometry.

The maximum mean action time may be rewritten in the form

$$t'_G = \frac{L^2 \Phi_G}{D_{\text{equiv}}}, \tag{34}$$

where the equivalent diffusivity is the log mean of the extreme values taken by the nonlinear diffusivity,

$$D_{\text{equiv}} \equiv \frac{D_{\text{wet}} - D_{\text{dry}}}{\ln(D_{\text{wet}}/D_{\text{dry}})}, \tag{35}$$

where

$$D_{\text{wet}} \equiv D_0 e^{\delta M_1}, \quad D_{\text{dry}} \equiv D_0 e^{\delta M_0}. \tag{36}$$

Even though the moisture penetration problem is a nonlinear diffusion one, the definition used for mean action time justifies the treatment of the diffusion of moisture as an equivalent linear diffusion problem, at least in terms of the times taken to wet grains. That is, the form of equation (34) is the same as the time-scaling obtained with a linear diffusion equation with a diffusion equal to D_{equiv}.

A simple extension that allows for the swelling of the grain is to imagine that the swelling happens relatively fast, so that the main effect is to increase grain size, slowing down the wetting of the interior. An upper limit on wetting time is obtained by considering the time to wet a grain that is larger by a factor equal to the total swelling that takes place. For example, if grain volume increases by a factor 1.5, then length increases by a factor $1.5^{1/3}$, and mean wetting time increases by a factor of $1.5^{2/3} \approx 1.3$.

A more sophisticated treatment of grain swelling as a moving boundary problem using the concept of mean action time has some fundamental difficulties – the mean action time then varies with time, corresponding to each point in the grain moving in space. So the following section uses different, asymptotic, methods to deal with grain swelling.

3.2 Asymptotic Analysis — Swelling Model

In order to gain some insight into the movement of water when there is swelling, we derive an approximate solution in a region of parameter space of physical interest. We consider the case where the moisture content is changed substantially, and in particular where the resulting water diffusivities at the initial M_0 level and at the final M_1 level are an order of magnitude different. Under such circumstances, because the diffusivity is such a strong function of the moisture content, water penetrates the grain as a steep front. Approximately steady-state flux conditions occur in the highly conductive hydrolyzed outer zone, there is little moisture transfer in the inner core, and the two zones are separated by a steep front whose position is determined by the flux in the outer zone. This concept is the same as that underlying the shrinking core model of Suzuki *et al* (1977), although here it is motivated by the strongly nonlinear diffusivity $D = D_0 e^{\delta M}$.

An infinite cylindrical grain model will be used here. Since the aspect ratio for grains of interest is of the order of 2 to 1 (or greater) this model represents the grain geometry and the physics of moisture uptake better than either spherical or plate models. These cases can be solved in the same way as considered here for the cylindrical model.

For the non-dimensional cylindrical model the absorbing external surface area of the grain is $2\pi R(t)$ where $R(t)$ is the radius of the expanding grain. The grain

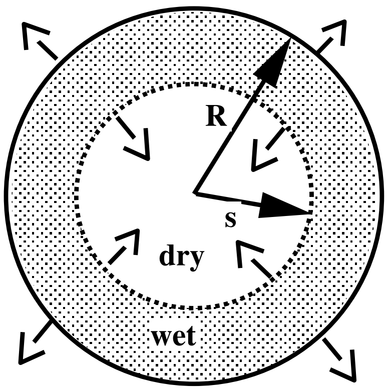

Figure 3: Sketch of the cylindrical model

surface is taken to be initially at the position $R = 1$, since length L has been scaled out of the problem. The model is sketched in figure (3).

The problem is then

$$\frac{\partial}{\partial t}\left(\frac{\alpha + m}{\gamma + \nu m}\right) = \nabla \cdot \left(\frac{e^{\beta m}\nabla m}{(\gamma + \nu m)^2}\right) \quad , \tag{37}$$

with

$$\begin{aligned} m &= -1 \text{ at } t = 0 \quad , & (38)\\ m &= 0 \text{ at } r = R(t) \quad , & (39)\\ \frac{\partial m}{\partial r} &= 0 \text{ at } r = 0 \quad , & (40)\\ \frac{dR}{dt} &= \frac{\nu}{\gamma}\frac{\partial m}{\partial r} \quad , & (41)\\ R(0) &= 1 \quad . & (42) \end{aligned}$$

Because the parameter β is in the exponential it has a significant influence on the solution and the approximate solution described below can be generated by performing a large activation energy asymptotic analysis on the system in the limit $\beta \to \infty$.

The approximate solution is found by breaking the solution into two main regions. The inner region has $0 \le r < s(t)$ and is where no additional water has

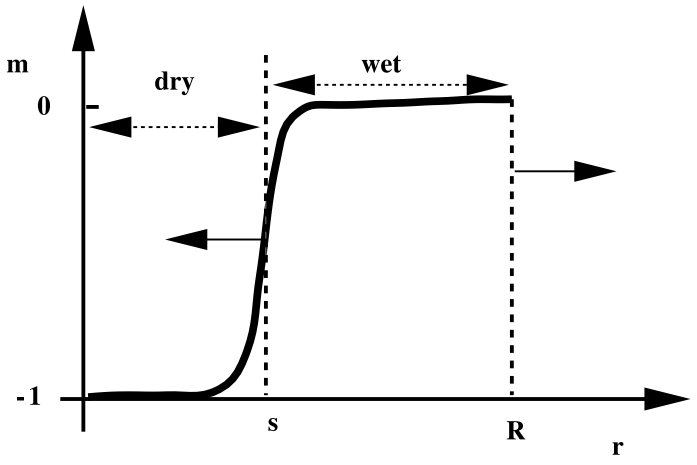

Figure 4: Sketch showing notation for wetting front and outer grain surface.

diffused while the outer region $s(t) < r \leq R(t)$ is where the flux is nearly constant. The interface between these regions is designated by $s(t)$, and is the wetting front, which has a surface area of $2\pi s(t)$ per unit length of cylinder.

In the outer wetted region (see figure (4)) $s(t) < r < R(t)$ the steady-state diffusion equation

$$\nabla\cdot\left(\frac{e^{\beta m}\nabla m}{(\gamma+\nu m)^2}\right) = 0, \qquad (43)$$

governs the moisture profile. In cylindrical coordinates this integrates to give

$$G(m) = A(t)\ln(r) + B(t), \text{ where } G(m) = \int_{-1}^{m} \frac{e^{\beta y}}{(\gamma+\nu y)^2}dy. \qquad (44)$$

Thus, after satisfying moisture conditions at the grain surface and front ($m = 0$ at $r = R(t)$ and $m = -1$ at $r = s(t)$), the following implicit moisture profile description in the wetted region is obtained:

$$G(m) = G(0)\left(\frac{\ln(r/s)}{\ln(R/s)}\right), \qquad (45)$$

where the locations of the expanded grain surface $R(t)$ and the front $s(t)$ are yet to be determined. These functions must also be chosen so that the solution satisfies the boundary condition at the outer boundary and mass conservation at the wetting front. Hence the boundary condition requires

$$\frac{dR(t)}{dt} = \frac{\nu}{\gamma}\frac{\partial m}{\partial r}(R(t), t) \ . \tag{46}$$

To generate the mass conservation equation that holds across the narrow wetting front, we multipy equation (37) by r and integrate across the wetting front from $r = s^-$ to $r = s^+$ to get

$$\int_{s^-}^{s^+} r \frac{\partial}{\partial t}\left(\frac{\alpha + m}{\gamma + \nu m}\right) dr = \left[\frac{e^{\beta m}}{(\gamma + \nu m)^2} r \frac{\partial m}{\partial r}\right]_{s^-}^{s^+} \ . \tag{47}$$

Interchanging the time derivative and the spatial integration gives

$$\begin{aligned} \frac{\partial}{\partial t}\left(\int_{s^-}^{s^+} r\left(\frac{\alpha + m}{\gamma + \nu m}\right) dr\right) \quad &- \quad \frac{ds^+}{dt} s^+ \left(\frac{\alpha + m(s^+)}{\gamma + \nu m(s^+)}\right) + \frac{ds^-}{dt} s^- \left(\frac{\alpha + m(s^-)}{\gamma + \nu m(s^-)}\right) \\ &= \quad \left[\frac{e^{\beta m}}{(\gamma + \nu m)^2} r \frac{\partial m}{\partial r}\right]_{s^-}^{s^+} \ . \end{aligned} \tag{48}$$

We now make some approximations based on the fact that the diffusivity is a rapidly changing function of moisture. Namely we let s^+ and s^- tend towards the value at the wetting front, $s(t)$; ahead of the wetting front (r near s^-) we assume the moisture remains at $m \approx -1$ and there is no diffusive flux on this side of the front; while behind the moisture front (r near s^+) the rapid diffusion makes the moisture content there nearly uniform with $m \approx 0$ and the moisture flux is $\partial G/\partial r$ at $s(t)$. These approximations can then be used to eliminate the integral in equation (48) and yield the condition

$$F\frac{ds(t)}{dt} = -\frac{\partial G}{\partial r}(m(s(t))) \ , \tag{49}$$

where

$$F \equiv \left(\frac{\alpha}{\gamma} - \frac{\alpha - 1}{\gamma - \nu}\right) \ . \tag{50}$$

We now solve equations (46) and (49) subject to the initial conditions $R(0) = 1$ and $s(0) = 1$. In solving the problem it will be useful to note that

$$\frac{\partial G}{\partial r} = \frac{G(0)}{r \ln(R(t)/s(t))} = \frac{e^{\beta m}}{(\gamma + \nu m)^2}\frac{\partial m}{\partial r}$$

We find that

$$\begin{aligned}
\frac{dR(t)}{dt} &= \frac{G(0)}{ER(t)\ln(R(t)/s(t))} \ , & (51)\\
\frac{ds(t)}{dt} &= -\frac{G(0)}{Fs(t)\ln(R(t)/s(t))} \ , & (52)
\end{aligned}$$

where

$$E \equiv 1/(\nu\gamma) \ . \tag{53}$$

Dividing equation (51) by (52) we obtain

$$\frac{dR}{ds} = -\frac{F}{E}\frac{s}{R} \ , \tag{54}$$

so that

$$R^2 + \frac{F}{E}s^2 = 1 + \frac{F}{E} \ , \tag{55}$$

that is, s can be found explicitly as a function of R,

$$s \equiv S(R) = \sqrt{\frac{E}{F}}\sqrt{1 + \frac{F}{E} - R^2} \ , \tag{56}$$

after applying the initial conditions. This explicit connection between the size of the dry grain core during water uptake and the swollen grain size is a direct consequence of the steady state profile assumption and material conservation. By the time the front reaches the core the grain radius will reach the value

$$R_f = \sqrt{1 + \frac{F}{E}} \ . \tag{57}$$

The grain will continue to absorb water until completely saturated, but the additional time required for completion is implicitly assumed to be negligible in this asymptotic approach.

With $S(R)$ now determined, equation (51) can be integrated to obtain the following implicit expression for $R(t)$:

$$\int_1^R R' \ln(R'/S(R'))dR' = \frac{G(0)}{E}t \ , \tag{58}$$

The integral evaluates to give

$$4G(0)t = ER^2 \ln R^2 + [F + E(1 - R^2)] \ln \left(1 + \frac{E}{F}(1 - R^2)\right) \ . \tag{59}$$

The largest R can be is when the argument of the ln function is zero, giving $(R^2 - 1) = F/E$. This corresponds to $s = 0$ in equation (55).

The dimensionless time for moisture to fully penetrate a cylindrical grain (when $s = 0$) then becomes

$$t^* = \frac{(E + F)}{4G(0)} \ln \left(\frac{E + F}{E}\right) \ . \tag{60}$$

The penetration time in seconds is then given by

$$t^*_{\text{swelling}} = \frac{L^2}{D_0} e^{-\delta M_1} \frac{(E + F)}{4G(0)} \ln \left(\frac{E + F}{E}\right) \ . \tag{61}$$

Note that the form of this wetting time is the same as without swelling, relating time to the square of the length. The new feature is the dependence on E, F and $G(0)$, which in turn depend in a moderately complicated way on ρ_w, ρ_s, M_0 and M_1. In the limit $\rho_w \to \infty$, we recover the same expression for maximum penetration time as in the non-swelling case, equation (32) with $\Phi_G = 1/4$.

Note also that for large β, Laplace's method applied to the various integrals gives the leading behaviour $G(0) \sim 1/(\beta\gamma^2)$ as $\beta \to \infty$. This approximation can be quite good even when β is only 5, as illustrated in Figure 5. The thin line shows $G(0)$ when $\gamma = 1.8$ and $\nu = 0.65$, while the thick line shows $G(0)\beta\gamma^2$, which is close to one when the leading behaviour is a good approximation.

4 Asymptotic Analysis — Swelling and Cooking Model

This model is directed at steam batch-processes with a temperature above gelatinisation temperature rapidly established (by conduction) throughout the grain, and moisture penetrating more slowly. At these high temperatures it is

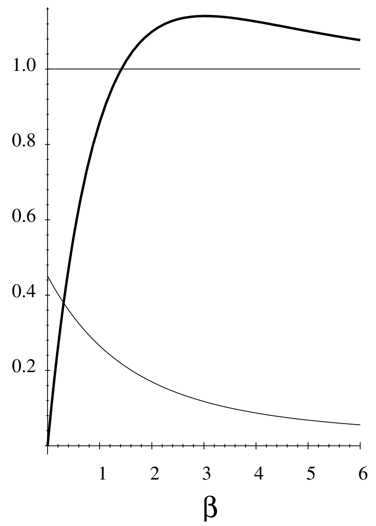

Figure 5: Sketch showing dependence of $G(0)$ on β. The thin curve is $G(0)$, the heavy curve is $G(0)\beta\gamma^2$, and the thin line shows the value 1.

expected that gelatinisation is taking place at or very near to the wetting front. In fact, Stapley (1995) notes that the evidence from experimental studies of grain cooking is that the wetting front coincides with gelatinisation.

Again a cylindrical grain model will be examined and the effects of both swelling due to moisture uptake and gelatinisation will be taken into account.

At the wetting front virgin starch is irreversibly gelatinised by water transported from the grain's surface. Inside this front there is insufficient water to cause gelatinisation, while outside this front there is no more virgin starch — it is all gelatinised. This sets up the problem with the usual Stephan conditions with the one difference that the critical water content at which irreversible gelatinisation takes place is temperature dependent (see Figure 1). So the wetting front is now locked onto the moisture content at which gelatinisation occurs, which depends on temperature. Furthermore, mass conservation at the wetting front is replaced by a requirement that enough moisture enters the front to maintain this moisture content. We have

$$M(s(t), t) = M_G(T) \ , \tag{62}$$

where $r = s(t)$ is the location of the front, and T is the (known) constant grain temperature.

The swelling grain model (15) is assumed to describe moisture transport from the grain surface to the front (with possibly different diffusion coefficients), and any additional swelling at this front is assumed to be negligible. The flux of water supplied by diffusion through the already gelatinised region to the front has to be sufficient to feed the gelatinisation reaction. The volume flux density $(m^3/(m^2 s)$ of water relative to axes fixed in space is given by equations (9) and (13),

$$\mathbf{u}_w = D_0 e^{\delta M} \left(\frac{\phi - 1}{M} \right) \nabla M \quad , \tag{63}$$

so that at $s(t)$

$$f \frac{ds}{dt} = -D_0 e^{\delta M} \left(\frac{1 - \phi}{M} \right) \nabla M \ . \tag{64}$$

The stoichiometric number f is the volume of water needed to bring unit volume of virgin starch from the initial moisture content M_0 up to the gelatinisation moisture content M_G. f is then given by

$$f = (M_G - M_0)\rho_s/\rho_w \ . \tag{65}$$

Using the same scaling as in section 2.2.2, and again dropping the over-bars on the non-dimensional terms, the front conditions become

$$m(s(t)) = m_g(T) \quad , \tag{66}$$

and

$$f \frac{ds}{dt} = -e^{\beta m_g} \frac{\partial m}{\partial r}(s(t)) \frac{1}{(\gamma + \nu m_g)(\alpha + m_g)} \quad , \tag{67}$$

where in non-dimensional terms

$$f = \nu(m_g + 1) \quad . \tag{68}$$

Since gelatinisation controls or holds up the process, an almost steady state moisture profile is expected in the outer region, and the analysis continues in a similar fashion to that presented in the previous section for a swelling grain below the gelatinisation temperature. The moisture profile is given by

$$G(m) - G(0) = [G(m_g) - G(0)] \frac{\ln(r/R)}{\ln(s/R)}, \tag{69}$$

and now

$$\frac{dR(t)}{dt} = \frac{\nu}{\gamma} \frac{\partial m}{\partial r}(R(t)) \tag{70}$$

determines the location of the expanded grain surface. The resulting equations for $(R(t), s(t))$ are given by

$$\frac{dR(t)}{dt} = \frac{G(0) - G(m_g)}{ER(t) \ln(R/s)} \ , \tag{71}$$

and

$$\frac{ds(t)}{dt} = -\frac{G(0) - G(m_g)}{F_G s(t) \ln(R/s)} \ , \tag{72}$$

where

$$F_G \equiv \frac{\nu(m_g + 1)(\alpha + m_g)}{\gamma + \nu m_g} \ , \tag{73}$$

and integration gives the time to gelatinise

$$t_g = \frac{E}{G(0) - G(m_g)} \int_1^R r \ln \left[\frac{r}{s(r)} \right] dr. \tag{74}$$

As in section (3.2), the integral evaluates to give

$$4[G(0) - G(m_g)]t = ER^2 \ln(R^2) + \left[F_G + E(1 - R^2) \right] \ln \left[1 + \frac{E}{F_G}(1 - R^2) \right] \ , \tag{75}$$

and

$$1 - s^2 = \frac{E}{F_G}(R^2 - 1) \ . \tag{76}$$

Except for the new definition of F_G, which replaces F, the model for swelling with gelatinisation at the wetting front is almost identical to the model for swelling with no gelatinisation. Detailed model comparisons follow in the Discussion section.

δ	8.6
M_1	0.6
M_0	0.15
ρ_s	1400 kg/m^3
ρ_w	992 kg/m^3

Table 2: Parameter values used to compare models.

5 Discussion

The three models are first compared here using the parameter values listed in Table (2), and using dimensionless values of s, R and t. The same value of δ is used to allow direct comparison in the dimensionless case.

The location of the non-dimensional wetting front $s(t)$ predicted by each of the three models is plotted in figure (6). The heavy line is the nonswelling result (33), the dashed line is the swelling result (60), and the thin line is the cooking and swelling result (75), with the choice $m_g = -0.5$. In the rest of this discussion, the cooking and swelling model is referred to simply as the cooking model.

Note the large (undefined) initial velocity of the wetting front seen in both the swelling and cooking models. This leads to more rapid initial moisture penetration in the swelling and cooking models.

This may seem surprising at first sight, since we expect the inclusion of swelling in a model to slow down moisture penetration. However, the rapid initial velocities are not a feature of swelling, but of the cylindrical geometry and the method of solution used in the swelling and cooking models. This becomes clearer when the swelling model solution for $s(t)$ is plotted for values of ρ_w increasing from 992 (the thickest dashed line) to 50000 (the thinnest dashed line), in figure (7). Larger values of ρ_w give almost the same curve as the value $50,000$. Note that the singularity at $t = 0$ persists to the limit of large ρ_w, which is the non-swelling limit of the swelling model. The difference between this limit and the mean action time nonswelling solution is the method of analysis and the treatment of the wetting front. Note that in the graph, the time for total grain penetration is the same for the nonswelling model and the large ρ_w limit of the swelling model, as the analysis after equation (61) predicts.

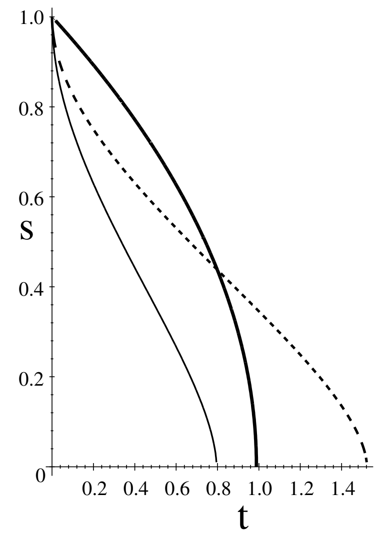

Figure 6: Non-dimensional wetting front locations $s(t)$ for the three models, non-swelling (thick line), swelling (dashed line) and cooking with $m_g = -0.5$ (fine line).

At later times, using $\rho_w = 992$, the nonswelling model front overtakes the swelling front in figure (6), as expected. The cooking model remains the fastest, but this is due to the assumption used in the plot that gelatinisation takes place at $m_g = -0.5$. Other choices for m_g can make the cooking model the slowest of all, as illustrated in figure (8).

The curve with $m_g = -0.9$ is the fastest to wet/cook, because little moisture is assumed to be required to gelatinise the starch. Cook times increase smoothly as m_g increases in equal increments to -0.1. The choice $m_g = -0.29$ gives a cooking $s(t)$ that coincides almost exactly with the swelling model curve, confirming the similarity of the two models, with a match obtained when the moisture required by stoichiometry in the cooking model to advance the wetting front a given distance, is equal to the moisture required by mass conservation in the swelling model.

Note also the almost linear regions in the swelling and cooking models. These are not present if the analysis is limited to a one-dimensional geometry. Linear penetration rates are significant in the dissolution of polymers, and more is said

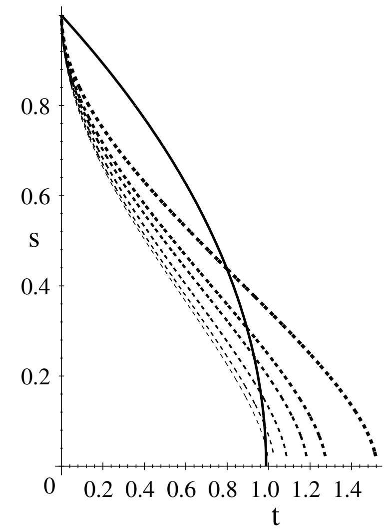

Figure 7: Non-dimensional wetting front locations $s(t)$ for the mean action time nonswelling model (solid curve), compared with $s(t)$ for the swelling model with increasing ρ_w (dashed curves). The righmost dashed curve has $\rho_w = 992$ as in the previous figure, then proceeding to the left the values of ρ_w are 2000, 3000, 6000, 15000 and 50000 for each dashed curve.

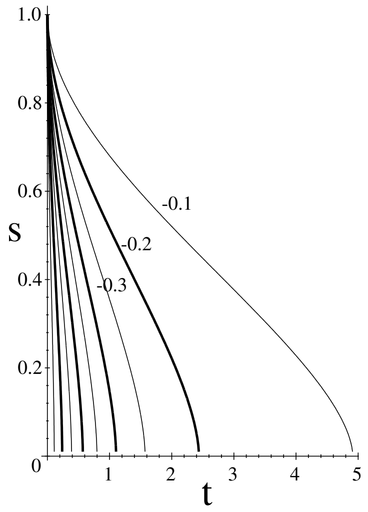

Figure 8: Non-dimensional wetting front locations $s(t)$ for the cooking model, for values of m_g from -0.1 to -0.9 in equal decrements of -0.1. Only a few of the m_g are annotated, as the curves change smoothly as m_g changes.

about this below.

The non-dimensional outer grain surface location $R(t)$ in each model is presented in figure (9), using the parameter values listed in Table (2). The nonswelling model has $R = 1$, the swelling model is the dashed curve, and the cooking model (with $m_g = -0.5$) is the thin curve. The longer distance moved by the swelling model grain surface is due mainly to the assumed value $m_g = -0.5$ for the cooking model — the distances moved by the grain surfaces in the swelling and the cooking models are equal when $m_g = -0.29$.

Equation (45) in combination with equations (55) and (59) implicitly give $m(r, t)$ for the swelling model. The moisture levels calculated using Maple satisfying these equations are plotted against r for a selection of times in figure (10). Times used are an initial time of 0.05, then equal increments of 0.2 up to a time of 1.85. The wetting profiles are reassuringly steep, consistent with the assumptions used in the analysis, and the almost linear rate of penetration is also clearly apparent.

The model curves $s(t)$ in the dimensional case are presented in figure (11). As

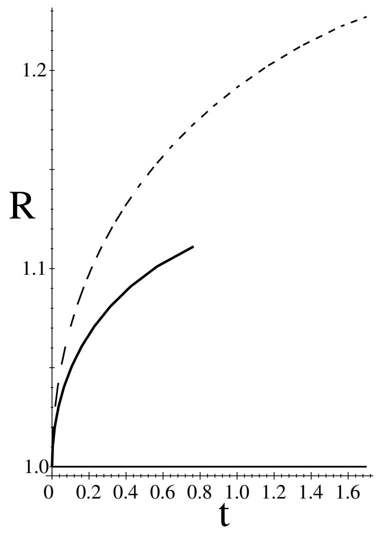

Figure 9: Non-dimensional grain surface locations $R(t)$ for the nonswelling model ($R = 1$), the swelling model (dashed curve), and the cooking model (heavy curve).

discussed previously, for the non-swelling model we take $\delta = 8.6$ and $D_0 = 1.5 \times 10^{-11}$ m^2/s; for the other two models we take $\delta = 10.8$ and $D_0 = 1.6 \times 10^{-11}$ m^2/s. The cooking model again has $m_g = -0.5$.

With these choices of differing parameter values, the slowest model is the nonswelling one, due to the effect of fitting a larger exponent in the diffusivity for the other two models. The times given here are indicative only, since we have used a grain size consistent with long-grain rice, but the diffusivity model and parameter values are for corn kernels. Substantial fitting and verification with experiments like that conducted in Syarief *et al* (1987) would be needed to obtain realisitic estimates for actual whole cereal grains.

Stapley *et al* (1997a) present moisture profiles versus depth for wheat grain wetting at temperatures above gelatinisation, obtained using NMR imaging techniques. Steamed grains have uniform and steadily rising moisture content. Grains immersed in boiling water feature sharp moisture fronts, preceded however by significant moisture levels. They find that the Thomas-Windle model (Thomas and Windle, 1982) gives better fits to the sharp moisture profiles than

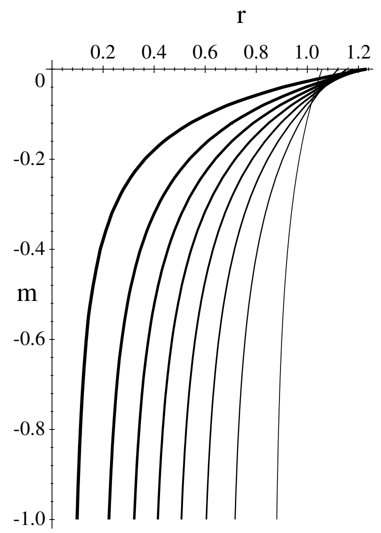

Figure 10: Moisture profiles $m(r, t)$ calculated for the swelling model. m is plotted against r, for various time values, starting with $t = 0.05$ for the thinnest curve nearest $r = 1$, then with equal time increments of 0.2 up to $t = 1.85$ for the thickest curve, when moisture has nearly fully penetrated the cylindrical grain.

the other diffusive models they tried, including linear models and nonlinear power-law models. A key feature of the Thomas-Windle model is that it gives a linear relationship between penetration depth and time, developed to explain *anomalous diffusion* or *Type II Diffusion* in the movement of solvent into polymers.

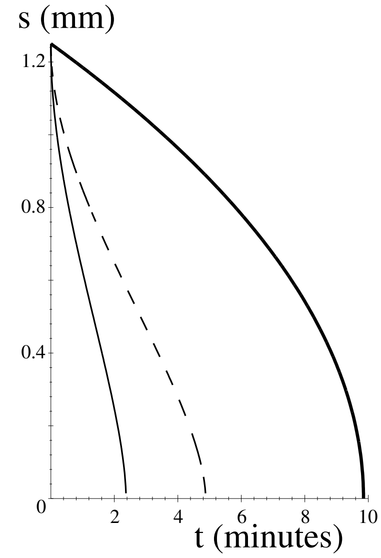

Figure 11: Wetting or cooking front locations (mm versus minutes) for the non-swelling model (thick curve), the swelling model (dashed curve), and the cooking model (thin curve).

The present work with (much simpler) nonlinear diffusion equations gives steep moisture fronts, due to the nonlinear diffusivity. It also gives regions of almost linear moisture penetration rates, at intermediate times, for both the swelling and cooking models, so offers a promising alternative to the rather complicated Thomas-Windle model. Another promising approach is to consider the effect of a low diffusivity grain skin on moisture penetration (Landman and Please, 1998). More work is needed, in the form of NMR experiments and numerical analysis, to improve confidence in mathematical models of whole grain cooking, to allow the fitting of different diffusivities for different types of grain, and to investigate temperature effects on nonlinear diffusivity. NMR techniques offer a promising method, since they resolve front locations in the grain.

Acknowledgements

The research reported in this paper arose from a problem presented by Uncle Tobys Company Ltd to the 1996 Mathematics-in-Industry Study Group (MISG) held at the University of Melbourne. There is a report on the initial modelling in McGowan and McGuinness (1996). The authors wish to thank the organizers of this meeting for providing such a stimulating research environment, especially the director Dr. Kerry Landman, and the following academics and students for contributing their expertise and energies as part of the team that tackled the problem: Ellis Cumberbatch, Eugeni Donskoi, Duncan Gray, James Gunning, Kerry Landman, Steve Mirams, Irene Pestov, Camelo Pisani, Yvonne Stokes, Nick Stokes, David White and Steve White.

References

Bakshi, A.S. and Singh, R.P. (1982), Modelling Rice Parboiling Process, *Lebensm.-Wiss. und Technol,* **15** pp.89–92.

Bear, J. (1972) Dynamics of Fluids in Porous Media, Dover, NY.

Broadbridge, P. (1990), Infiltration in saturated swelling soils and slurries: exact solutions for constant supply rate, *Soil Science,* **149** No. 1 (Jan 1990) pp.13–22.

King, J.R. (1989), The isolation oxidation of Silicon — the reaction controlled case, *Siam J. Appl. Math.,* **49** pp.1064–1080.

Landman, K.A. and Please, C. (1998), Modelling Moisture Uptake in a Cereal Grain, submitted to *I.M.A. J. Math. App. Bus. Ind.*

McGowan, P. and McGuinness, M. (1996), Modelling the Cooking Process of a Single Cereal Grain, in the proceedings of *The 1996 Mathematics-in-Industry Study Group,* held at the University of Melbourne, Melbourne, Australia, 29 Jan – 2 Feb 1996, Ed John Hewitt, pp.114–140.

McNabb, A. (1975), Asymptotic behaviour of solutions of a Stephan problem, *J. Math. Anal. and App.,* **51** pp.633–642.

McNabb, A. and Wake, G.C. (1991), Heat conduction and finite measures for transition times between steady states, *IMA Journal of Mathematics,* **47** pp.193–206.

Philip, J.R. (1969), Hydrostatics and hydrodynamics in swelling soils, *Water Resources Research,* **5** No. 5 (Oct 1969) pp.1070–1077.

Smiles, D.E. and Rosenthal, M.J. (1968), The movement of water in swelling materials, *Aust. J. Soil Res.,* **6** pp.237–248.

Stapley, A.G.F. (1995), Phd Thesis, University of Cambridge, England, 1995.

Stapley, A.G.F., Fryer, P.J. and Gladden, L.F. (1997a), *Models for processing of whole wheat grains in cereal manufacture* in Proc. 7th Int. Congress on Engineering and Food, Brighton, UK, 1997, pp.H37–H40.

Stapley, A.G.F. and Fryer, P.J. (1997b), *Steam cooking of wheat and rice grains: a model for simultaneous heat and mass transfer*, in Proc. 7th Int. Congress on Engineering and Food, Brighton, UK, 1997, pp.C57–C59.

Suzuki, K., Kubota, K. and Hosaka, H. (1977), Studies on the Cooking Rate Equations of Rice, *J. Food Science,* **42** No. 6 pp.1545–1548.

Syarief, A.M., Gustafson, R.J. and Morey, R.V. (1987), Moisture diffusion coefficients for yellow-dent corn components, *Trans. American Soc. of Agricultural Engineers,* **30** pp.522–528.

Thomas, N.L. and Windle, A.H. (1982), A theory of Case II diffusion, *Polymer,* **23** April 1982, pp.529–542.

Zhang,T.-Y., Bakshi, A.S., Gustafson, R.J. and Lund, D.B. (1984), Finite Element Analysis of Nonlinear Water Diffusion During Rice Soaking, *J. Food Science* **49** pp.246–250,277.